J. Biochem. 2009;145(5)669–675
doi:10.1093/jb/mvp024

Over-Expression and Characterization of *Bacillus subtilis* Heme O Synthase

Tatsushi Mogi[1,2,*]

[1]*Department of Biomedical Chemistry, Graduate School of Medicine, the University of Tokyo, Hongo, Bunkyo-ku, Tokyo 113-0033; and* [2]*ATP System Project, ERATO, JST, Nagatsuta, Midori-ku, Yokohama 226-0026, Japan*

Received December 20, 2008; accepted January 31, 2009; published online February 9, 2009

Biosynthesis of heme A from heme B is catalysed by two enzymes, heme O and heme A synthases, in the membrane. Heme O synthase in *Bacillus subtilis* (CtaB) has eight transmembrane helices and catalyses the transfer of a farnesyl group from farnesyl diphosphate to the 2-vinyl group on pyrrole ring A of ferrous heme B. In this study, we constructed the overproduction system for the *B. subtilis* CtaB in *Escherichia coli*. We isolated His_7-CtaB by affinity chromatography and demonstrated the presence of the heme-binding site in heme O synthase. His_7-CtaB binds substoichiometric amounts of heme B and O, substrate and unreleased product, respectively. Mutagenesis studies suggest that strictly conserved His199 present at the extracellular side of helix 5 would serve as the heme-binding site. We are hoping that the overproducing system for heme O synthase would help understanding of detailed mechanism on heme O biosynthesis and X-ray crystallographic studies.

Key words: *Bacillus subtilis*, CtaB, heme A biosynthsis, heme O synthase, His-tag.

Abbreviations: HPLC, high-performance liquid chromatography; SML, sucrose monolaurate.

Hemes O and A (Fig. 1) are 'key compounds' of the aerobic respiration in mitochondria and bacteria and used for the dioxygen reduction site of the heme-copper terminal oxidases (*i.e.* cytochrome *c* oxidase and quinol oxidase) while heme D (chrolin) is preferred for the dioxygen reduction by bacterial *bd*-type quinol oxidase (*1*, *2*). Heme B (protoheme IX) is preferred as an electron-accepting heme and used as the dioxygen reduction site only in microaerobic cytochrome bb_3 and cbb_3 terminal oxidases (*1–3*). Hemes O and A carry a 17-hydroxyethylfarnesyl group at position 2 of pyrrole ring A (*4*, *5*). Heme A has a formyl group at position 8 of pyrrole ring D (*5*) and is derived from heme O. In *Escherichia coli*, we discovered that the last ORF (*cyoE*) in the cytochrome *bo* operon encodes heme O synthase (*6–8*). CyoE synthesizes and supplies heme O just enough for the heme *o*-Cu_B binuclear centre of cytochrome *bo*-type quinol oxidase (CyoABCD). Δ*cyoE* mutations eliminated completely heme O in the cytoplasmic membranes and resulted in a non-functional heme *bb*-type oxidase (*7–9*). On the basis of gene fusion studies, Chepuri and Gennis (*10*) proposed that CyoE has seven transmembrane helices. Alanine scan mutagenesis studies revealed the presence of a catalytic site in putative cytoplasmic loops 2/3 and 4/5 (*8*). We demonstrated that in the presence of Mg^{2+} or Ca^{2+} CyoE-overproduced membranes catalysed the transfer of a farnesyl group from farnesyl diphosphate to the 2-vinyl group on pyrrole ring A of ferrous heme B (*6*) (Fig. 1). We found also that the *cyoE* homologue (*ctaB*) in the *ctaA-ctaB-ctaCDEF* gene cluster of thermophilic *Bacillus* PS3 encodes a thermotolerant heme O synthesis (*11*). Thus, we concluded that the *cyoE*/*ctaB* gene, which is often associated with the bacterial oxidase operon, encodes a novel enzyme, heme O synthase. Mutational and expression studies on the *ctaB* gene in *Bacillus subtilis* (*12*, *13*) and *Bacillus cereus* (*14*, *15*) and the *COX10* gene in *Paracoccus denitrificans* (*16*), *Rhodobacter sphaeroides* (*17*), yeast (*18*, *19*) and human (*20*, *21*) reached to the same conclusion.

In *B. subtilis*, Svensson *et al.* (*12*, *13*, *22*) showed that the *ctaA* gene is involved in heme A biosynthesis where CtaA (heme A synthase) oxidizes the 8-methyl group of heme O to a formyl group (Fig. 1). CtaA homologue (Cox15p) in yeast (*23*, *24*) and human (*25*) plays a similar role in heme A synthesis. Brown *et al.* (*26*) expressed the *B. subtilis* CtaA and CtaB in *E. coli* (BL21/pET-3a:*ctaB*/pET-9d:*ctaA*) at some extent and determined structures of hemes produced in the cells. They postulated that CtaA catalyses the oxidation of the 8-methyl group to a formyl group through a C8 alcohol intermediate via successive P450-like monooxygenase reactions, as reported for chlorophyll *b* biosynthesis (*1*, *22*, *27*). Barros *et al.* (*24*, *28*) found in *Schizosaccharomyces pombe* that ferredoxin is fused at the *C*-terminus of CtaA and demonstrated that ferredoxin (Yah1p) and ferredoxin reductase (Arh1p) are required for heme A synthesis in yeast (*Saccharomyces cerevisiae*). These observations are consistent with the P450-like monooxygenase mechanism; however, hemes in CtaA are not coordinated by the sulphur atom of cysteines (*13*). The source of oxygen for the 8-formyl group has been considered as molecular oxygen, but Brown *et al.* (*29*) suggested that the dominant source of the oxygen atom in heme A is derived from H_2O.

*To whom correspondence should be addressed. Tel: +81-3-5841-8202, Fax: +81-3-5841-3444, E-mail: tmogi@m.u-tokyo.ac.jp

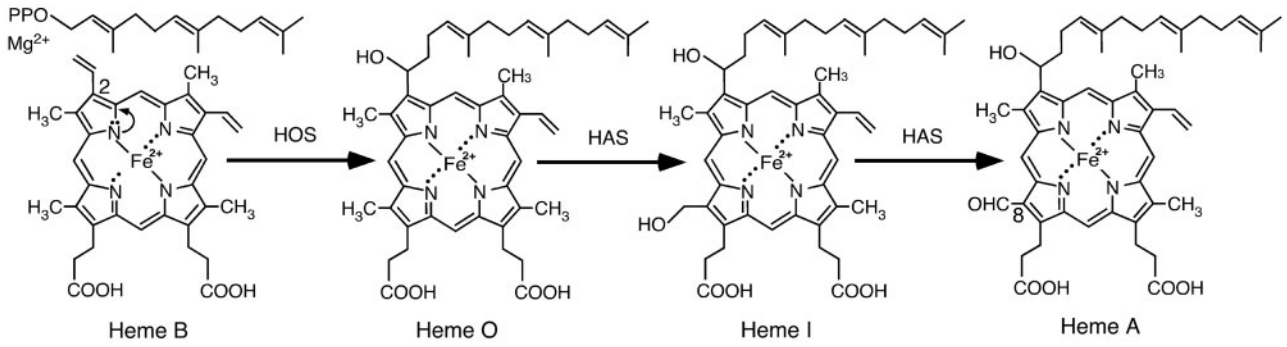

Fig. 1. **Biosynthesis of heme O and heme A.** Conversion of heme B to heme O is catalysed by HOS (heme O synthase), which is encoded by the *E. coli cyoE*, *Bacillus subtilis ctaB*, and mitochondrial *COX10* genes. HAS (heme A synthase), which is encoded by the *B. subtilis ctaA* and mitochondrial *COX15* genes, oxidizes heme O to heme A through heme I (8-hydroxymethyl derivative of heme O). PPO indicates a diphosphoryl group.

Svensson *et al*. (*13*, *22*) expressed the wild-type CtaA in *B. subtilis* and *E. coli* and found that the isolated CtaA binds only a substoichiometric amount (~0.4 mol) of low-spin heme b_{558}. It showed peaks at 428, 528 and 558 nm in the reduced state and at 414 nm in the oxidized state. No other redox metal centres were identified at a significant level. When co-expressed with heme O synthase (CtaB) in *B. subtilis*, they found that CtaA binds ~0.2 mol each of heme B and heme A and shows the α peaks at 558 and 585 nm, respectively, in the reduced state (*13*). Later, Sakamoto *et al*. (*30*) expressed the *Bacillus stearothermophilus* CtaA in *E. coli* (XL-1 blue/pUCctaA) and found the presence of substoichiometric amounts of heme B and A in cytochrome *ba*-type CtaA. It was assumed that heme A was unreleased product and that heme B was a cofactor for the activation of dioxygen. Svensson *et al*. (*13*, *22*) proposed that CtaA has originated by the result of tandem gene duplication and that conserved His60, His126, His 216 and His278 in transmembrane helices 2, 4, 6 and 8 (Fig. 2) serve as axial ligands for low-spin heme b_{558} (E_m, +85 mV) and a_{585} (+242 mV). Recently, Hederstedt *et al*. (*31*) carried out site-directed mutagenesis studies on invariant histidines present in the *B. subtilis* CtaA. They expressed Leu and Met mutants with the His_6-tag at the *C*-terminus in *B. subtilis* and identified mutant CtaA proteins except H216L in the membranes. The presence of cytochrome *a* in H60M, H216M, H278L and H278M indicates that these mutants retain fully or partially heme A synthase activity. They postulated that His123 is directly involved in catalysis and that His60 and His216 in the *N*- and *C*-terminal halves, respectively, are axial ligands for bound hemes. However, His60 is substituted by Asn in Actinomycetales like *Streptomyces* and *Mycobacterium* (*1*). Recently, we over-expressed the *B. subtilis* CtaA in *E. coli* and demonstrated the presence of two heme B-binding sites (*32*). Further, we found that heme binding was reduced to about half of the wild-type level in His216 and His278 mutants not in His60 and His123 mutants. These observations rather suggest that His216 and His278 are involved in heme binding. In contrast to heme A synthase, not much is known about heme O synthase. Overproduction of heme O or A could be used as a novel probe for heme-binding sites in transmembrane proteins (*3*).

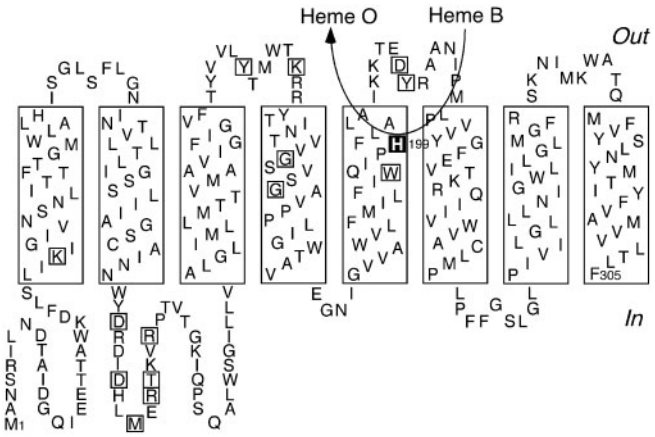

Fig. 2. **Topological model of heme O synthase (CtaB) from *B. subtilis*.** Putative transmembrane regions predicted by SOSUI (http://sosui.proteome.bio.tuat.ac.jp/sosuiframe0.html) are shown by 'rectangles'. Conserved residues in heme O synthase are marked by 'squares'.

In this study, we constructed the overproduction system for the *B. subtilis* His_7-CtaB and isolated for the first time heme O synthase. The isolated His_7-CtaB binds substoichiometric amounts of heme B and O, possibly a substrate and unreleased product, respectively. In our structure model for the *B. subtilis* CtaB (Fig. 2), which has eight transmembrane helices instead of seven in the Chepuri–Gennis model (*10*), a putative heme B ligand (His199) is located at the extra-cellular end of helix 5, now allowing the transfer of heme O to the extra-cellular catalytic site of heme A synthase (*13*, *22*, *31*) through a CtaAB heterodimer (*33*). As reported for the *E. coli* CyoE (*8*), H199A lost the ability to overproduce heme O in *E. coli*. We are hoping that the overproducing systems for heme O synthase (*3*, this study) and heme A synthase (*32*) would help understanding of detailed mechanism on heme O and A biosynthesis and their X-ray crystallographic studies.

MATERIALS AND METHODS

Cloning, Mutagenesis and Expression of CtaB Gene—Heme O synthase gene (*ctaB*, 978 nt) was amplified by PCR using the chromosomal DNA from *B. subtilis* strain IAM12119 (Institute of Molecular and Cellular Biosciences, University of Tokyo) with primers CtaBF (5′-CGCGCCGGATCCGAAGGAGATATAGAT ATGATAGAGTTGCAGGTTATTTTATTCTCCTGCGT-3′) and CtaBR (5′-GGGGGAATTCGGCCGGATCCTATTAGA AAAGCGTCAAGACAACCATGGCAACGAAATA-3′) and cloned into the *Bam*HI–*Eco*RI site of pET-3b (Novagen) to give pET-3b-ctaB. pET-15b-ctaB was constructed as follows. The *ctaB* gene on pET-3b-ctaB was amplified as a *Bam*HI–*Bgl*II fragment by PCR using primers CtaBPetF (5′-CGCCGGGATCCGATGGCTAACTCCAGA ATCTTAAATG-3′) and CtaBR3 (5′-ATACGGAAGCTTC TTGATCA TTATGATTGCCTGGATTCATAACG-3′) and sub-cloned into the *Bam*HI site of pET-15b (Novagen). Then, the *ctaB* gene was sub-cloned into the *Nde*I–*Hin*dIII of pQE2 (Qiagen) to give pQE2-ctaB. For the expression vector for the *ctaB* gene, we selected pQE2-ctaB because it showed the over-expression of CtaB in *E. coli* (data not shown). Substitution of His199 by Ala was introduced with QuickChange XL (Stratagene) using primers H199AF (5′-TTATTTATTTGGCAGATTCCTGC TTTCTTAGCATTGGCTATTAAG-3′) and H199AR (5′-CT TAATAGCCAATGCTAAGAAAGCAGGAATCTGCCAAAT AAATAA-3′). Nucleotide sequence of the entire wild-type and mutant genes was confirmed by DNA sequencing with 3100 Genetic Analyzer (Applied Biosystems, CA) with primers (T7 forward and T7 terminator (Novagen), CtaBPF (5′-GTGAGCGGATAACAATTATAATAGA-3′), CtaBPIF (5′-AAAGTAAGACCGACGGTTACGGGTAAA A-3′) and CtaBP1 (5′-CGGAGTCTTTACGTATGTTGTAT TGTAC-3′). For the expression of the ctaB gene, *E. coli* BL21 CodonPlus (DE3)-RIL (Novagen) was transformed with pQE2-ctaB, and then transformants were grown at 28°C overnight in L-broth supplemented with Overnight Express Autoinduction System 1 (Novagen), trace metals (*32*), 0.1 mg/ml Na-ampicillin (Sigma) and 0.2 mM 5-aminolevulinic acid (Wako Pure Chemicals, Osaka, Japan). The yield of cells was ~5 g wet weight per litre culture.

Isolation of His_7-CtaB by Affinity Chromatography—Cells were suspended in 50 mM Tris–HCl (pH 7.4) containing 10 mM Na-EDTA (pH 8), 0.5 mM phenylmethanelsulfonyl fluoride (Sigma), 0.5 mM benzamidine (Sigma) and 0.5 mg/ml egg white lysozyme (Sigma), incubated on ice for 30 min, and disrupted by sonication. After removal of unbroken cells and spheroplasts, cytoplasmic membranes were isolated by isopicnic sucrose density centrifugation (*33*). Proteins were solubilized from the membrane vesicles with 2.5% sodium *N*-lauroylsarcosine (MP Biomedicals, Aurora, OH) in 50 mM sodium phosphate (pH 7.4) containing 1 mM phenylmethanelsulfonyl fluoride by stirring for 30 min at 4°C. The mixture was centrifuged for 30 min at 100,000*g*. Supernatant was applied to a Ni–NTA His-Bind Superflow (Novagen) column (25 mm i. d. × 10 cm) equilibrated with buffer A (50 mM Na-phosphate (pH 7.4), 0.3 M NaCl and 0.1% SML) containing 10 mM imidazole (MP Biochemicals, Ohio). After washing with buffer A containing 10 mM imidazole, His_7-CtaB was eluted with buffer A containing 200 mM imidazole. Eluate was concentrated and desalted by ultrafiltration with Amicon Ultra-15 (50,000 MWCO, Millipore). Then, the CtaB-enriched fraction was applied to a Toyopearl AF-Chelate-650M (Tosoh, Tokyo, Japan) column (15 mm i. d. × 12 cm), and His_7-CtaB was eluted with a 0–250 mM linear gradient of imidazole in 50 mM sodium phosphate (pH 7.4) containing 0.3 M NaCl and 0.1% sucrose monolaurate (Mitsubishi-Kagaku Foods Co., Tokyo, Japan) at the flow rate of 3 ml/min. Purified enzymes were stored at –80°C until use.

Electrophoresis and Western Blotting Analysis—Twenty micrograms of cytoplasmic membrane proteins were subjected to 5–20% SDS–polyacrylamide gel electrophoresis, followed by western blotting analysis with rabbit anti-His-tag antibody (Medical Biological Lab., Nagoya, Japan). His_7-CtaB was visualized by using alkaline phosphatase-conjugated sheep anti-rabbit IgG (Chemicon Int., Temecula, CA, USA) or by staining with GelCode Blue Stain Reagent (Pierce).

Determinations of Heme and Protein Content and Heme Analysis—Heme B (*plus* O) content was determined by pyridine hemochromogen method, and protein concentration was determined with BCA Protein Assay Reagent (Pierce) (*34*). Hemes were extracted from the membranes or the purified enzyme with HCl-acetone and separated by reverse-phase high-performance liquid chromatography (HPLC) using an Altex Ultrashere ODS column (4.6 mm i. d. × 25 cm; Beckman Coulter) (*7*). The solvent was 95% ethanol/acetic acid/water (70:17:7, vol/vol), and the flow rate was 0.5 ml/min. The elution profile was monitored at 396 nm with an SPD-M10A_{VP} photodiode array detector (Shimadzu Co., Kyoto, Japan). Hemin (Sigma) and hemes B and O extracted from the *E. coli* cytochrome *bo*, heme A from bovine cytochrome *c* oxidase were used as standards.

Absorption Spectroscopy—Absorption spectra of the air-oxidized and sodium hydrosulphite reduced forms of His_7-CtaB in buffer A were determined with a V-550 UV/Vis spectrophotometer (JASCO, Tokyo, Japan) (*35*).

RESULTS AND DISCUSSION

Functional Over-Expression of His_7-CtaB in E. coli—For the over-expression of the *B. subtilis* CtaB in *E. coli*, we constructed pET-3b-ctaA, pET-15b-ctaB and pQE2-ctaB and examined the expression level of CtaB in different *E. coli* strains (BL21(DE3), BL21(DE3)/pLysS, BL21 CodonPlus(DE3)-RIL, Rosetta gamiB(DE3), and Origami(DE3) under different growth conditions (*i.e.* growth temperature, carbon source). Finally, we succeeded in the over-expression of the *B. subtilis* CtaB in BL21 CodonPlus(DE3)-RIL/pQE2-ctaB, which has been grown overnight at 28°C by using Overnight Express Autoinduction System 1 (Novagen). Five to 20 percent SDS–polyacrylamide gel electrophoresis analysis showed that a 30-kDa protein increased in cytoplasmic membranes upon the expression of His_7-CtaB with pQE2-ctaB (Fig. 3, lane 2). Western blotting analysis of cytoplasmic membranes with the anti-His-tag antibody identified the 30-kDa band as His_7-CtaB (Fig. 3, lane 5). Probably due

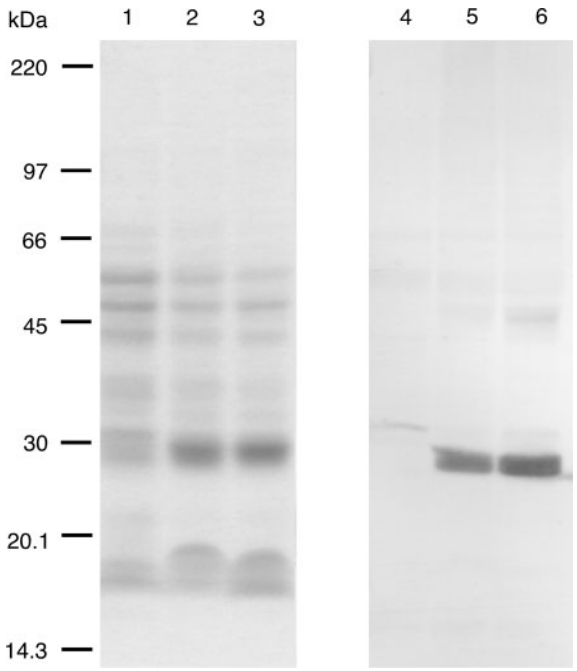

Fig. 3. **Western blot analysis of cytoplasmic membranes isolated from wild-type CtaB and H199A mutant with the anti-His-tag antibody.** Samples are: (1) and (4) vector control (BL21 CodonPlus-RIL (DE3)/pQE2), (2) and (5) wild- type (pQE2-ctaB) and (3) and (6) H199A (pQE2-ctaB-H199A). Twenty micrograms of membrane proteins were loaded per lane on 5–20% SDS–polyacrylamide gel. His_7-CtaB was visualized with GelCode (lanes 1–3) or alkaline phosphatase-conjugated second antibody (lanes 4–6).

Table 1. **Changes in properties of hemes present in cytoplasmic membranes upon the overproduction of CtaB in BL21 CodonPlus (DE3)-RIL/pQE2-ctaB.**

Plasmid	Heme content (nmol/mg protein)	Hemochrome (nm)	Heme B: Heme O
pQE2	3.02	556.0	91:9
pQE2-ctaB	1.65	552.5	44:56
pQE2-ctaB-H199A	2.92	556.0	ND*

*Not determined.

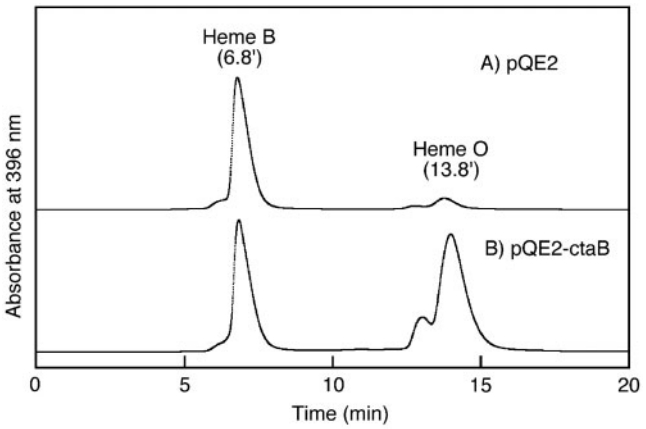

Fig. 4. **Reverse-phase HPLC analysis of hemes present in cytoplasmic membranes isolated from the control (BL21 CodonPlus-RIL (DE3)/pQE2) and the heme O synthase-expressing strain (BL21 CodonPlus-RIL (DE3)/pQE2-ctaB).**

to anomalous mobility of membrane proteins in SDS–polyacrylamide gels, apparent molecular mass (~30 kDa) was smaller than 35,751 Da for His_7-CtaB (*cf.* CtaB, 33,792 Da), which has been estimated from the DNA sequence. Similarly, apparent molecular mass for the *B. subtilis* CtaA (34,085 Da) and the *E. coli* CyoE (32,249 Da) have been estimated to be 23 kDa in Tricine–SDS–polyacrylamide gels (*22*) and 26 kDa in 12.5% SDS–polyacrylamide gels (*6*), respectively.

Upon the over-expression of His_7-CtaB, heme B (*plus* O) content was rather decreased to 1.65 from 3.02 nmol/mg membrane protein of the control strain, as found for the *E. coli* CyoE-overproducing strain (*3*). In the His_7-CtaB-overproducing strain, pyridine ferrohemochrome showed the absorption maximum for the α peak at 552.5 nm (Table 1), which is close to 552 nm of heme O (*1*). In the vector control strain, we found the α peak at 556 nm (Table 1), which is identical to that of heme B. Then, hemes were extracted from the membranes with acid acetone and subjected to reverse-phase HPLC analysis (Fig. 4). Heme B and heme O were eluted at 6.8 and 13.8 min, respectively. The overproduction of His_7-CtaB in BL21 CodonPlus (DE3)-RIL/pQE2-ctaB changed the relative heme O content in the cytoplasmic membranes to 56% from 9% in the vector control strain (Table 1), indicating the functional expression of the *B. subtilis* heme O synthase in *E. coli*. The increase in the relative heme O content was comparable to 58% in BL21 CodonPlus (DE3)-RIL/pQE2-cyoE and 83% in BL21(DE3)/pLysS/pTTQ18-cyoE (*3*).

Isolation of the Wild-Type His_7-CtaB by Affinity Chromatography—The *B. subtilis* CtaA and CtaB have similar molecular mass (34.1 *vs.* 33.8 kDa) and isoelectric points (9.5 *vs.* 9.6), but we found that CtaB tends to aggregate in non-ionic detergent (sucrose monolaurate) at low ionic strength. Thus, we solubilized cytoplasmic membranes by sodium *N*-lauroylsarcosine and partially purified His_7-CtaB by Ni-NTA affinity chromatography (Fig. 5, Table 2). Unlike His_6-CtaA in sucrose monolaurate (*32*), His_7-CtaB in anionic detergent did not bind tightly to a Ni–NTA His-Bind Superflow column and did not elute completely from the column probably due to the aggregation. Protein recovery at the Ni–NTA chromatography step was 5–7%. Then, pooled His_7-CtaB fractions were subjected to the second affinity chromatography with a Toyopearl AF-Chelate-650M column (Fig. 6). Upon the elution with a 0–250 mM linear imidazole gradient, we found two peaks corresponding to *b*-type cytochromes. His_7-CtaB was eluted at around 18 min (~75 mM imidazole) as a broad peak, as found for the *B. subtilis* CtaA (~70 mM) (*32*), and had the Abs412/Abs280 ratio of ~1.3. A small peak at around 4–5 min with the Abs412/Abs280 ratio of ~0.5 is likely contaminated cytochrome *bo*-type quinol oxidase. The isolated His_7-CtaB (Fig. 5, lane 6) contains a substoichiometric amount of hemes (0.135 mol/mol His_7-CtaB). Reverse-phase HPLC analysis of bound hemes showed the presence of heme O and heme B at a ratio of 0.77:0.23. Heme B is assumed to be

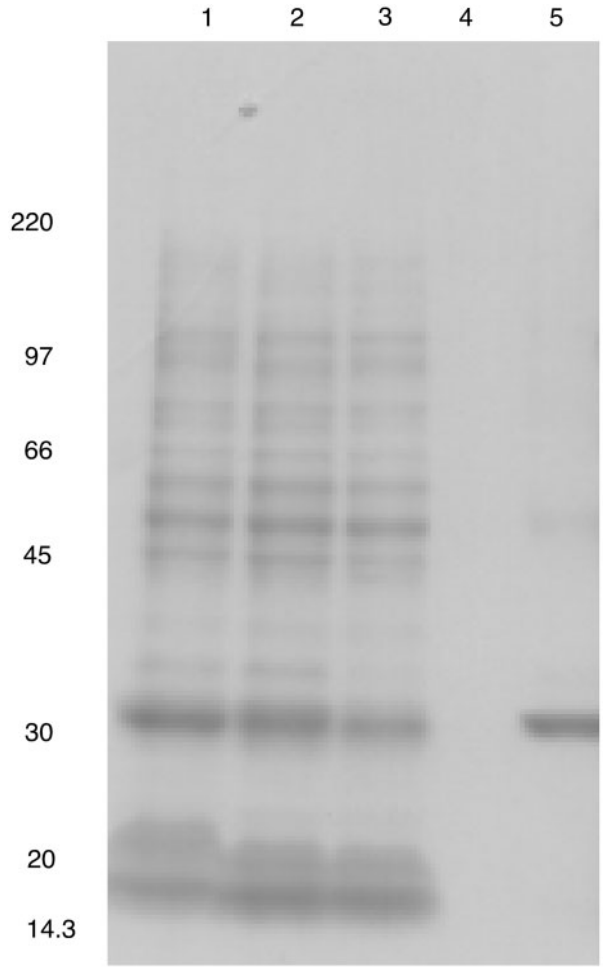

Fig. 5. **Isolation of the wild-type His_7-CtaB by Ni–NTA chromatography.** Samples are: (1) cytoplasmic membranes from BL21 CodonPlus-RIL (DE3)/pQE2-ctaB, (2) Na-lauroylsarcosine extract, (3) flow-through fractions, (4) unbound fractions washed with 10 mM imidazole and (5) bound fractions eluted with 200 mM imidazole from a Ni-NTA column. After 5–20% SDS–polyacrylamide gel electrophoresis, proteins were visualized with GelCode.

Table 2. **Isolation of the wild-type His_7-CtaB by affinity chromatography.**

Preparation	Protein (mg)	Heme (B+O) (μmol)	Heme content (nmol/mg protein)
Cytoplasmic membranes	1,395 (100%)	2.30 (100%)	1.65
Ni–NTA step	74 (5.3)	0.21 (9.1)	2.80
AF-Chelate-650M peak	23 (1.7)	0.09 (3.9)	3.78

a substrate and heme O appears to be an unreleased product of heme O synthase (Fig. 1). Substoichiometric amounts of bound hemes have been reported for the *B. subtilis CtaA* where ~0.2 mol each of heme B and A were bound to 1 mol CtaA (*13*). At room temperature, His_7-CtaB showed peaks at 423, 528 and 556 nm in the

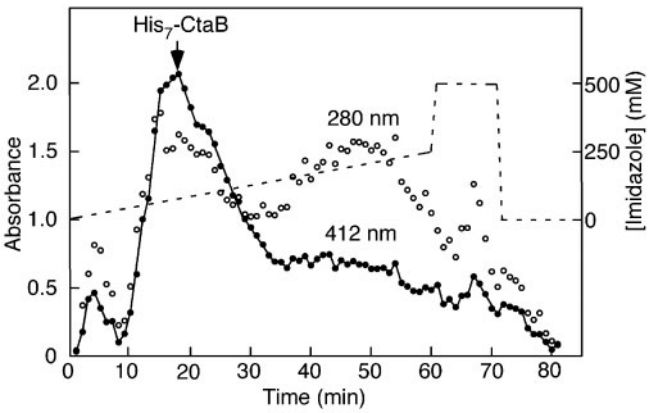

Fig. 6. **Elution profile of His_7-CtaB on Toyopearl AF-Chelate-650M affinity chromatography.** CtaB fractions eluted from a Ni–NTA column were applied on a Toyopearl AF-Chelate-650M column, and His_7-CtaB was eluted with a 0–250 mM linear gradient of imidazole in 50 mM Na-phosphate (pH 7.4), 0.3 M NaCl and 0.1% sucrose monolaurate. Elution profiles of proteins and cytochromes were monitored at 280 (open circle) and 412 (closed circle) nm, respectively.

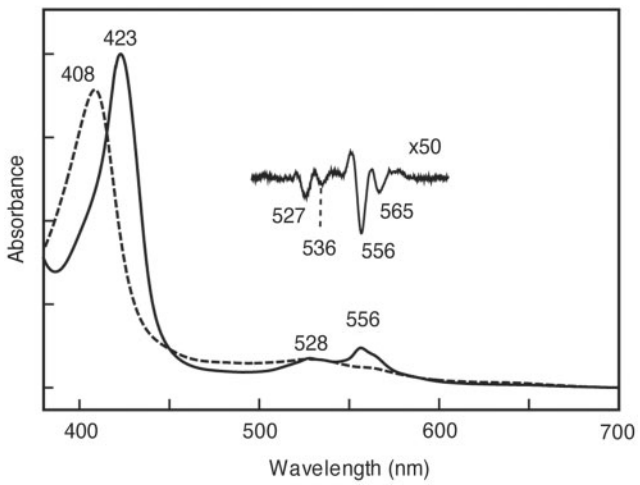

Fig. 7. **Absorption spectra of the air-oxidized (broken line) and fully reduced (solid line) forms of purified His_7-CtaB.** Absolute spectra of His_7-CtaB (10 μM heme B *plus* O) were recorded in 50 mM Na-phosphate (pH 7.4) containing 0.3 M NaCl and 0.1% sodium *N*-lauroylsarcosine before and after reduction with Na-hydrosulphite. Inset: the second-order finite difference spectrum of the α and β peak region of the reduced form.

fully reduced state and at 408 and 528 nm in the air-oxidized state (Fig. 7). A broad feature at around 630 nm in the air-oxidized from indicates the presence of a high-spin species. In the second-order finite difference spectrum of the reduced form, the α and β peaks split into 556 and 565 nm and 527 and 536 nm, respectively. The relative peak area for the α peak (70:30) was comparable to the heme B: heme O ratio. Peak splitting may be related to the heterogeneity of bound hemes in His_7-CtaB.

Structure of the B. subtilis CtaB and the Role of Conserved His199—On the basis of gene fusion

experiments and hydropathy analysis, Chepuri and Gennis (*10*) proposed a structure model for the *E. coli* heme O synthase (CyoE). It consists of seven transmembrane helices, and strictly conserved His199 is placed in large cytoplasmic loop 4/5. Among conserved residues in the CtaB/CyoE/Cox10p family, His199 is the only one candidate for the heme B-binding site. On the contrary, the catalytic site(s) of heme A synthase is assumed to be present at the extra-cellular side of transmembrane helices (*13*, *22*, *33*). Thus, it is difficult to carry out heme A biosynthesis within a putative heme O synthase/heme A synthase heterodimer (*33*). We examined the structure of the *B. subtilis* CtaB with SOSUI (*36*) and PSIPRED (*37*) and found the presence of eight putative transmembrane regions. In our structure model for the *B. subtilis* CtaB (Fig. 2), His199 is placed at the extra-cellular side of helix 5, allowing the transfer of heme O to heme A synthase at the same side of the cytoplasmic membranes. Such orientations of the catalytic sites in heme O and heme A synthases are consistent with the heme binding sites in the heme-copper terminal oxidases (*38–41*).

Saiki *et al*. (*8*) carried out alanine scan mutagenesis studies and found that Ala substitutions of Trp195, Pro198, His199, Asp210 and Tyr211 (*i.e*. *B. subtilis* CtaB numbering) within or near helix 5 eliminated the heme O synthase activity, indicating the importance of the His199 region for the catalytic activity. To examine the role of His199 in the *B. subtilis* CtaB, we constructed and characterized the H199A mutant. Western blotting analysis of cytoplasmic membranes with the anti-His-tag antibody showed that H199A mutation did not affect the expression level of His_7-CtaB (Fig. 3, lanes 3 and 6). Heme B (+O) content in the membranes was returned to the control level, and the α peak of pyridine ferrochrome at 556.0 nm indicates the loss of heme O synthase activity (Table 1).

Conclusion—In this study, we constructed the over-expression system for the *B. subtilis* CtaB in *E. coli* and demonstrated the presence of the heme-binding site in heme O synthase (Table 2, Figs 6 and 7). Mutagenesis studies on the *B. subtilis* CtaB (this study) and on the *E. coli* CyoE (*8*) suggest that strictly conserved His199 present at the extra-cellular side of helix 5 would serve as the heme-binding site. We are hoping that the over-producing systems for heme O synthase (this study) and heme A synthase (*32*) would help understanding of detailed mechanism on heme O and A biosynthesis and their X-ray crystallographic studies.

ACKNOWLEDGEMENTS

I thank Eri Mizuochi-Asai, Takahiro Watanabe-Nakayama, Sachiko Endou, and Satoru Akimoto (ERATO, JST) for technical assistance.

FUNDING

This work was supported in part by Grant-in-Aid for Scientific Research (C) (20570124) and Creative Scientific Research (18GS0314) from the Japan Society for the Promotion of Science.

CONFLICT OF INTEREST

None declared.

REFERENCES

1. Mogi, T. (2003) Biosynthesis and role of heme O and heme A. in *The Porphyrin Handbook* (Kadish, K., Guilard, R., and Smith, K., eds.) Vol. 17, pp. 157–181, Academic Press, San Diego
2. Mogi, T., Minagawa, J., Hirano, T., Sato-Watanabe, M., Tsubaki, M., Uno, T., Hori, H., Nakamura, H., Nishimura, Y., and Anraku, Y. (1998) Substitutions of conserved aromatic amino acid residues in subunit I perturb the metal centers of the *Escherichia coli bo*-type ubiquinol oxidase. *Biochemistry* **37**, 1632–1639
3. Mogi, T. (2009) Effects of replacement of low-spin heme *b* by heme O on *Escherichi coli* cytochrome *bo* and *bd* quinol oxidases. *J. Biochem.* **145** (doi: 10.1093/jb/mvp015)
4. Puustinen, A. and Wikström, M. (1991) The heme groups of cytochrome *o* from *Escherichia coli*. *Proc. Natl Acad. Sci. USA* **88**, 6122–6126
5. Caughey, W.S., Smythe, G.A., O'Keeffe, D.H., Maskasky, J.E., and Smith, M.I. (1975) Heme A of cytochrome *c* oxidase. Structure and properties: comparisons with hemes B, C, and S and derivatives. *J. Biol. Chem.* **250**, 7602–7622
6. Saiki, K., Mogi, T., Ogura, K., and Anraku, Y. (1993) *In vitro* heme O synthesis by the *cyoE* gene product from *Escherichia coli*. *J. Biol. Chem.* **268**, 26041–26045
7. Saiki, K., Mogi, T., and Anraku, Y. (1992) Heme O biosynthesis in *Escherichia coli*: The *cyoE* gene in the cytochrome *bo* operon encodes a protoheme IX farnesyltransferase. *Biochem. Biophys. Res. Commun.* **189**, 1491–1497
8. Saiki, K., Mogi, T., Hori, H., Tsubaki, M., and Anraku, Y. (1993) Identification of the functional domains in heme O synthase: site-directed mutagenesis studies on the *cyoE* gene of the cytochrome *bo* operon in *Escherichia coli*. *J. Biol. Chem.* **268**, 26927–26934
9. Hill, J., Goswitz, V.C., Calhoun, M., García-Horsman, J.A., Lemieux, L., Alben, J.O., and Gennis, R.B. (1992) Demonstration by FTIR that the *bo*-type ubiquinol oxidase of *Escherichia coli* contains a heme-copper binuclear center similar to that in cytochrome *c* oxidase and the proper assembly of the binuclear center requires the *cyoE* gene product. *Biochemistry* **31**, 11435–11440
10. Chepuri, V. and Gennis, R. B. (1990) The use of gene fusions to determine the topology of all of the subunits of the cytochrome *o* terminal oxidase complex of *Escherichia coli*. *J. Biol. Chem.* **265**, 12978–12986
11. Saiki, K., Mogi, T., Ishizuka, M., and Anraku, Y. (1994) An *Escherichia coli cyoE* gene homologue in thermophilic *Bacillus* PS3 encodes a thermotolerant heme O synthase. *FEBS Lett.* **351**, 385–388
12. Svensson, B., Lübben, M., and Hederstedt, L. (1993) *Bacillus subtilis* CtaA and CtaB function in haem A biosynthesis. *Mol. Microbiol.* **10**, 193–201
13. Svensson, B., Andersson, K.K., and Hederstedt, L. (1996) Low-spin heme A in the heme A biosynthetic protein CtaA from *Bacillus subtilis*. *Eur. J. Biochem.* **238**, 287–295
14. Del Arenal, I.P., Contreras, M.L., Svlateorova, B.B., Rangel, P., Lledías, F., Dávila, J.R., and Escamilla, J.E. (1997) Haem O and a putative cytochrome *bo* in a mutant of *Bacillus cereus* impaired in the synthesis of haem A. *Arch. Microbiol.* **167**, 24–31
15. Contreras-Zentella, M., Mendoza, G., Membrillo-Hernández, J., and Escamilla, J.E. (2003) A novel double heme substitution produces a functional bo_3 variant of the

quinol oxidase aa_3 of *Bacillus subtilis*. *J. Biol. Chem.* **278**, 31473–31478
16. Steinrücke, P., Gerhus, E., and Ludwig, B. (1991) *Paracoccus denitrificans* mutants deleted in the gene for subunit II of cytochrome *c* oxidize also lack subunit I. *J. Biol. Chem.* **266**, 7676–7681
17. Cao, J., Hosler, J., Shapleigh, J., Revzin, A., and Ferguson-Miller, S. (1992) Cytochrome aa_3 of *Rhodobacter sphaeroides* as a model for mitochondrial cytochrome *c* oxidase. The *coxII/coxIII* operon codes for structural and assembly protein homologues to those in yeast. *J. Biol. Chem.* **267**, 24273–24278
18. Nobrega, M.P., Nobrega, F.G., and Tzagoloff, A. (1990) *COX10* codes for a protein homologous to the *ORF1* product of *Paracoccus denitrificans* and is required for the synthesis of yeast cytochrome oxidase. *J. Biol. Chem.* **265**, 14220–14226
19. Tzagoloff, A., Nobrega, M., Gorman, N., and Sinclair, P. (1993) On the function of the yeast *COX10* and *COX11* gene products. *Biochem. Mol. Biol. Int.* **31**, 593–598
20. Valnot, I., von Kleist-Retzow, J.-C., Barrientos, A., Gorbatyuk, M., Rustin, P., Tzagoloff, A., Rotig, A., and Munnich, A. (1999) A mutation in the human *COX10* gene for heme A:farnesyl transferase causes cytochrome oxidase deficiency. *Hum. Mol. Genet.* **9**, 1245–1249
21. Antonicka, H., Leary, S.C., Agar, J.N., Horvath, R., Kennaway, N.G., Harding, C.O., Jaksch, M., and Shoubridge, E.A. (2003) Mutations in *COX10* result in a defect in mitochondrial heme A biosynthesis and account for multiple, early-onset clinical phenotypes associated with isolated COX deficiency. *Hum. Mol. Genet.* **12**, 2693–2702
22. Svensson, B. and Hederstedt, L. (1994) *Bacillus subtilis* CtaA is a heme-containing membrane protein involved in heme A biosynthesis. *J. Bacteriol.* **176**, 6663–6671
23. Glerum, D.M., Muroff, I., Jin, C., and Tzagoloff, A. (1997) *COX15* codes for a mitochondrial protein essential for the assembly of yeast cytochrome oxidase. *J. Biol. Chem.* **272**, 19088–19094
24. Barros, M.H., Carlson, C.G., Glerum, D.M., and Tzagoloff, A. (2001) Involvement of mitochondrial ferredoxin and Cox15p in hydroxylation of heme O. *FEBS Lett.* **492**, 133–138
25. Antonicka, H., Mattman, A., Carlson, C.G., Glerum, D.M., Hoffbuhr, K. C., Leary, S.C., Kennaway, N.G., and Shoubridge, E.A. (2003) Mutationsin *COX15* produce a defect in the mitochondrial heme biosynthetic pathway, causing early-onset fatal hypertrophic cardiomyopathy. *Am. J. Hum. Genet.* **72**, 101–114
26. Brown, K.R., Allan, B.A., Do, P., and Hegg, E.L. (2002) Identification of novel hemes generated by heme A synthase: evidence for two successive monooxygenase reactions. *Biochemistry* **41**, 10906–10913
27. Oster, U., Tanaka, R., Tanaka, A., and Rüdiger, W. (2000) Cloning and functional expression of the gene encoding the key enzyme for chlorophyll *b* biosynthesis (CAO) from *Arabidopsis thaliana*. *Plant J.* **21**, 305–310
28. Barros, M.H., Nobrega, F.G., and Tzagoloff, A. (2002) Mitochondrial ferredoxin is required for heme A synthesis in *Saccharomyces cerevisiae*. *J. Biol. Chem.* **277**, 9997–10002
29. Brown, K.R., Brown, B.M., Hosgland, E., Mayne, C.L., and Hegg, E.L. (2002) Heme A synthase does not incorporate molecular oxygen into the formyl group of heme A. *Biochemistry* **43**, 8616–8624
30. Sakamoto, J., Hayakawa, A., Uehara, T., Noguchi, S., and Sone, N. (1999) Cloning of *Bacillus stearothermophilus ctaA* and heme A synthesis with the CtaA protein produced in *Escherichia coli*. *Biosci. Biotechnol. Biochem.* **63**, 96–103
31. Hederstedt, L, Lewin, A., and Throne-Holst, M. (2005) Heme A synthase enzyme functions dissected by mutagenesis of *Bacillus subtilis* CtaA. *J. Bacteriol.* **187**, 8361–8369
32. Mogi, T. (2009) Probing structure of heme A synthase from *Bacillus subtilis* by site-directed mutagenesis. *J. Biochem.* **145** (doi: 10.1093/jb/mvp017)
33. Brown, B.M., Wang, Z., Brown, K.R., Cricco, J.A., and Hegg, E.L. (2004) Heme O synthase and heme A synthase from *Bacillus subtilis* and *Rhodobacter sphaeroides* interact in *Escherichia coli*. *Biochemistry* **43**, 13541–13548
34. Mogi, T., Minagawa, J., Hirano, T., Sato-Watanabe, M., Tsubaki, M., Uno, T., Hori, H., Nakamura, H., Nishimura, Y., and Anraku, Y. (1998) Substitutions of conserved aromatic amino acid residues in subunit I perturb the metal centers of the *Escherichia coli bo*-type ubiquinol oxidase. *Biochemistry* **37**, 1632–1639
35. Mogi, T., Akimoto, S., Endou, S., Watanabe-Nakayama, T., Mizuochi-Asai, E., and Miyoshi, H. (2006) Probing the ubiquinol-binding site in cytochrome *bd* by site-directed mutagenesis. *Biochemistry* **45**, 7924–7930
36. Hirokawa, T., Seah, B.C., and Mitaku, S. (1998) SOSUI: classification and secondary structure prediction system for membrane proteins. *Bioinformatics* **14**, 378–379
37. McGuffin, L.J., Bryson, K., and Jones, D.T. (2000) The PSIPRED protein structure prediction server. *Bioinformatics* **16**, 404–405
38. Iwata, S., Ostermeier, C., Ludwig, B., and Michel, H. (1995) Structure at 2.8 Å resolution of cytochrome *c* oxidase from *Paracoccus denitrificans*. *Nature* **376**, 660–669
39. Abramson, J., Riistama, S., Larsson, G., Jasaitis, A., Svensson-Ek, M., Laakkonen, L., Puustinen, A., Iwata, S., and Wikström, M. (2000) The structure of the ubiquinol oxidase from *Escherichia coli* and its ubiquinone binding site. *Nature Struct. Biol.* **7**, 910–917
40. Soulimane, T., Buse, G.P., Bourenkov, H.D., Bartunik, R., Huber, R., and Than, M.E. (2000) Structure and mechanism of the aberrant ba_3-cytochrome *c* oxidase from *Thermus thermophilus*. *EMBO J.* **19**, 1766–1776
41. Yoshikawa, S., Shinzawa-Itoh, K., Nakashima, R., Yaono, R., Yamashita, E., Inoue, N., Yao, M., Fei, M.J., Libei, C.P., Mizushima, T., Yamaguchi, H., Tomizaki, T., and Tsukihara, T. (1998) Redox-coupled crystal structural changes in bovine heart cytochrome *c* oxidase. *Science* **280**, 1723–1729